ISSN 1674-1056
http://cpb.iphy.ac.cn
http://iopscience.iop.org/cpb
中国物理 B
Chinese Physics
中国物理 Chinese Physics B

Calculation of electric field-temperature (*E*, *T*) phase diagram of a ferroelectric liquid crystal near the SmA-SmC$^{\alpha*}$ transition

F Trabelsi, H Dhaouadi, O Riahi, T Othman
Citation: Chin. Phys. B . 2018, 27(3): 037701. **doi:** 10.1088/1674-1056/27/3/037701

Journal homepage: http://cpb.iphy.ac.cn; http://iopscience.iop.org/cpb

What follows is a list of articles you may be interested in

Field-induced phase transitions in chiral smectic liquid crystals studied by the constant current method

H Dhaouadi, R Zgueb, O Riahi, F Trabelsi, T Othman
Chin. Phys. B . 2016, 25(5): 057704. **doi:** 10.1088/1674-1056/25/5/057704

Preparation and characterization of $Sr_{0.5}Ba_{0.5}Nb_2O_6$ glass-ceramic on piezoelectric properties

Shan Jiang(姜珊), Xuan-Ming Wang(王炫明), Jia-Yu Li(李佳宇),Yong Zhang(张勇), Tao Zheng(郑涛), Jing-Wen Lv(吕景文)
Chin. Phys. B . 2016, 25(3): 037701. **doi:** 10.1088/1674-1056/25/3/037701

Ultrahigh frequency tunability of aperture-coupled microstrip antenna via electric-field tunable BST

Du Hong-Lei, Xue Qian, Gao Xiao-Yang, Yao Feng-Rui, Lu Shi-Yang, Wang Ye-Long, Liu Chun-Heng, Zhang Yong-Cheng, Lü Yue-Guang, Li Shan-Dong
Chin. Phys. B . 2015, 24(12): 127704. **doi:** 10.1088/1674-1056/24/12/127704

Temperature dependences of ferroelectricity and resistive switching behavior of epitaxial $BiFeO_3$ thin films

Lu Zeng-Xing, Song Xiao, Zhao Li-Na, Li Zhong-Wen, Lin Yuan-Bin, Zeng Min, Zhang Zhang, Lu Xu-Bing, Wu Su-Juan, Gao Xing-Sen, Yan Zhi-Bo, Liu Jun-Ming
Chin. Phys. B . 2015, 24(10): 107705. **doi:** 10.1088/1674-1056/24/10/107705

Preparation and piezoelectric properties of potassium sodium niobate glass ceramics

Jiang Shan, Wang Xuan-Ming, Li Jia-Yu, Zhang Yong, Zheng Tao, Lv Jing-Wen
Chin. Phys. B . 2015, 24(6): 067701. **doi:** 10.1088/1674-1056/24/6/067701

Calculation of electric field–temperature (E, T) phase diagram of a ferroelectric liquid crystal near the SmA–SmC$^*_\alpha$ transition

F Trabelsi, H Dhaouadi[†], O Riahi, and T Othman

Université de Tunis El-Manar, Faculté des Sciences de Tunis, Laboratoire de physique de la matière molle et de modélisation électromagnétique (LP3ME), Campus Universitaire Farhat Hached 2092 *Tunis Tunisie*

(Received 11 September 2017; revised manuscript received 23 November 2017; published online 13 February 2018)

In this work we perform a theoretical calculation in order to reconstitute the (E–T) phase diagram of a chiral smectic liquid crystal in the vicinity of the SmA–SmC$^*_\alpha$ transition. This reconstruction is carried out on the basis of a thermodynamic calculation of the slope of the curve joining the SmC$^*_\alpha$ domain and the unwound SmC*. An empiric correction of the mean field term of Landau De-Gennes development is necessary to accomplish this reconstruction. Thereafter, an experimental validation is performed to verify our calculations.

Keywords: field-temperature phase diagram, liquid orystal

PACS: 77.84.-s, 77.80.-e, 77.80.B- **DOI:** 10.1088/1674-1056/27/3/037701

1. Introduction

Ferroelectric liquid crystals (FLC) have been intensively studied for several decades. A large number of investigations have been performed to improve our fundamental understanding of these crystals and to develop technological applications.[1] The chiral smectic phases of liquid crystals are layered structures, in which the rod-like molecules are lined up within the smectic layers. In the order of decreasing temperature and increasing tilt angle θ, one can observe a subset of the following full sequence:[2–5]

$$\text{I-SmA} - \text{SmC}^*_\alpha - \text{SmC}^* - \text{SmC}^*_{\text{FI2}} - \text{SmC}^*_{\text{FI1}} - \text{SmC}^*_{\text{A}} - \text{K}.$$

Some of these phases may sometimes be missing, but the order of appearance is conserved. Recently, an additional phase smectic-C^*_{d6} with a six-layer unit cell was discovered.[6]

In these materials, phase transitions can also be induced by the application of an external electric field.[7–9]

For all tilted mesophases, the application of an external electric field causes the destruction of the helicoidal structure. This can be described as a transition towards the unwound SmC* state.

Often, these transitions occur in two stages. An intermediate phase of a polar nature appears. The structure of this phase was the subject of several theoretical and experimental studies.[5,10–12] All these works describe a mesh with three layers, for this intermediate phase, similar to that of the SmC$^*_{\text{Fi1}}$ phase.

To describe the state of a chiral smectic sample, it is necessary to establish the electric field–temperature (E, T) phase diagram. Several works using different experimental techniques have been performed in this regard.[7,14,15]

A careful observation of these diagrams reveals the resemblance of the shapes of the borders between the domains of the different phases. This prompted us to undertake a theoretical study in an attempt to identify the equations which describe these borders. Such an analysis facilitates the complete reconstruction of a phase diagram based on the knowledge of a few experimental points.

The Landau De-Gennes theory treats only the transitions induced by a change of temperature.[16,17] Consideration of the energetic terms corresponding to an electric field and the polarization state, makes it possible to explain certain phenomena such as the electroclinic effect.[18] To study the field-induced phase transitions in these materials, it is necessary to exploit some classical thermodynamic results. These results will enable us to construct certain borders of the (E, T) phase diagram. In the vicinity of the SmA–SmC$^*_\alpha$ transition, borders rebuilding requires the introduction of an empirical correction that affects the mean-field term of the free energy development.

The first part of this work is devoted to classical thermodynamic study, which will facilitate the calculation of the slope of the curve joining the SmC$^*_\alpha$ domain and the unwound SmC*. In the second part, we introduce an empirical correction of the mean-field term of the Landau De-Gennes development. This correction makes it possible to complete the tracing of the border joining the domain of the SmC$^*_\alpha$ and the SmA. (E, T) diagrams of the product ($C_{10}F_3$) in the vicinity of the SmA–SmC$^*_\alpha$ transition. An experimental validation of the results of this study is proposed in the third section, where the (E, T) phase diagram of the product ($C_{10}F_3$[7,19]) is investigated.

[†]Corresponding author. E-mail: hassen.dhaouadi@ipeit.rnu.tn

© 2018 Chinese Physical Society and IOP Publishing Ltd

2. Phase transitions in electric systems and classical thermodynamic approach

2.1. Thermodynamic potential

The succession of phases, obtained by varying the temperature in a given thermodynamic system, can be attributed to a competition between the internal energy U of the system which is minimal for an ordered state at low temperature, and the entropy S which favors the disorder at higher temperature. The Helmholtz free energy $F = U - TS$ is the appropriate thermodynamic potential for studying the phase equilibrium of the system. For electrical systems such as chiral smectic liquid crystals, in which certain mesophases have a polar character and thus exhibit spontaneous polarization, the appropriate thermodynamic potential to study the field transitions is the Gibbs function,

$$F^* = U - TS - ED. \tag{1}$$

During a transformation of the system, the variation of the Gibbs potential is written as

$$\mathrm{d}F^* = -S\mathrm{d}T - D\mathrm{d}E, \tag{2}$$

where E represents the intensive state variable and D is the associated extensive state variable related to the unit of volume.[20]

The thermodynamic equilibrium of the system is expressed by the Gibbs relation

$$\mathrm{d}F^* = 0. \tag{3}$$

2.2. Boundaries equations

The curves which separate two domains in the (E,T) phase diagram correspond to an equilibrium of two phases. During an elementary displacement of one of these curves, the two phases coexist and remain in equilibrium. We then have

$$\mathrm{d}F_1^* = \mathrm{d}F_2^*. \tag{4}$$

From this relation we can determine the slope of the tangent at a point on this curve as

$$\alpha = \left(\frac{\mathrm{d}E}{\mathrm{d}T}\right)_{\mathrm{curv}} = \frac{S_1 - S_2}{D_2 - D_1}, \tag{5}$$

where (S_1, D_1) and (S_2, D_2) are the entropy and dielectric excitation in phases (1) and (2), respectively.

Experimentally D_1 and D_2 can be measured, however, the expression $S_1 - S_2 = -\Delta S$ is problematic. This requires a calculation of the entropy for each phase at zero field and at constant fields.

Note that

$$S = -\left(\frac{\mathrm{d}F^*}{\mathrm{d}T}\right)_E, \tag{6}$$

$$F_1^*(E,T) - F_1^*(0,T) = -\left(\frac{D_1^2}{2\varepsilon_1}\right) + \left(\frac{P_1 D_1}{\varepsilon_1}\right). \tag{7}$$

Taking the partial derivative with respect to T, we obtain

$$\begin{aligned} &S_1(D_1,T) - S_{01}(0,T) \\ &= -\left[-\frac{D_1}{\varepsilon_1}\left(\frac{\partial D_1}{\partial T}\right)_E + \frac{D_1^2}{2\varepsilon_1^2}\left(\frac{\partial \varepsilon_1}{\partial T}\right)_E \right. \\ &\quad + \frac{D_1}{\varepsilon_1}\left(\frac{\partial P_1}{\partial T}\right)_E + \frac{P_1}{\varepsilon_1}\left(\frac{\partial D_1}{\partial T}\right)_E \\ &\quad \left. - \frac{P_1 D_1}{\varepsilon_1^2}\left(\frac{\partial \varepsilon_1}{\partial T}\right)_E\right]. \end{aligned} \tag{8}$$

When $\varepsilon(T)$ is a constant for a homogeneous phase, we have

$$\left(\frac{\partial D_1}{\partial T}\right)_E = \left(\frac{\partial P_1}{\partial T}\right)_E. \tag{9}$$

If we suppose that $S_{01}(0,T) = S_{02}(0,T)$, we obtain

$$\begin{aligned} &S_1(E,T) - S_2(E,T) \\ &= \frac{1}{2\varepsilon_2}\left(\frac{\partial P_2^2}{\partial T}\right)_E - \frac{1}{2\varepsilon_1}\left(\frac{\partial P_1^2}{\partial T}\right)_E. \end{aligned} \tag{10}$$

Finally, we have the expression of the slope

$$\begin{aligned} \alpha &= \left(\frac{\partial E}{\partial T}\right)_{\mathrm{curve}} \\ &= \frac{s_1 - s_2}{D_2 - D_1} == \frac{1}{[(\varepsilon_2 E + P_2) - (\varepsilon_1 E + P_1)]} \\ &\quad \times \left[\frac{1}{2\varepsilon_2}\left(\frac{\partial P_2^2}{\partial T}\right)_E - \frac{1}{2\varepsilon_1}\left(\frac{\partial P_1^2}{\partial T}\right)_E\right]. \end{aligned} \tag{11}$$

This expression is simplified if the dielectric permittivity does not change in value during the transition $\varepsilon_1 = \varepsilon_2$. The expression of the slope can then be written as

$$\begin{aligned} \alpha &= \left(\frac{\partial E}{\partial T}\right)_{\mathrm{curve}} = \frac{s_1 - s_2}{D_2 - D_1} \\ &= \frac{1}{2\varepsilon(P_2 - P_1)}\left(\frac{\partial (P_2^2 - P_1^2)}{\partial T}\right)_E. \end{aligned} \tag{12}$$

In the general case where $\varepsilon_1 \neq \varepsilon_2$, we must consider equation (11). Fortunately, we can continue the analysis in a certain range of values of E to express D as a linear function of E, i.e. $D = \varepsilon E$ (we mean $\varepsilon_\perp$).

In the same way we calculate the entropy of the two phases and obtain an expression for the slope of the tangent at a given point on the curve as

$$\begin{aligned} &F_2^*(D_1,T) - F_2^*(0,T) \\ &= -ED_1 = -\frac{D_1^2}{2\varepsilon_1}, \end{aligned} \tag{13}$$

$$\begin{aligned} &S_1(T,D) - S_{01}(T,0) \\ &= -\left(-\frac{D_1}{\varepsilon_1}\left(\frac{\partial D_1}{\partial T}\right)_E + \frac{D_1^2}{2\varepsilon_1^2}\left(\frac{\partial \varepsilon_1}{\partial T}\right)_E\right), \end{aligned} \tag{14}$$

where $(\partial D_1/\partial T)_{D_1} = 0$ when D_1 is constant.

Supposing $S_{01}(0,T) = S_{02}(0,T)$, we obtain

$$s_1(D_1,T) - s_2(D_2,T) = -\frac{E^2}{2}\left(\frac{\partial(\varepsilon_1-\varepsilon_2)}{\partial T}\right)_V. \quad (15)$$

Finally, the slope of the tangent at a point of the curve is written as

$$\alpha = \left(\frac{\partial E}{\partial T}\right)_{\text{curve}} = \frac{s_1 - s_2}{D_2 - D_1} = \frac{E}{2(\varepsilon_1-\varepsilon_2)}\left(\frac{\partial(\varepsilon_1-\varepsilon_2)}{\partial T}\right)_V. \quad (16)$$

3. Mean-field theory and field induced phase transitions

3.1. Landau De-Gennes model of phase transitions

The Landau theory is a theory which examines the phenomenon accompanying phase transitions in systems where there is a symmetry break. Physically, we characterize the symmetry of a given phase by an order parameter. If the variation of this parameter during a phase transition takes place in a continuous manner, then this transition is called a second order transition. If it occurs in a discontinuous manner, it is a first order transition.

According to the Landau model, theoretical analysis of the transition SmA $\rightarrow$ SmC non-chiral was first proposed by Blinc.[21] Indenbom and Al[22] extended this analysis to the case of the transition SmA $\rightarrow$ SmC* chiral. In the smectic A (SmA), the molecular director is oriented perpendicular to the planes of the layers at an angle θ, and the normal of the smectic planes appears in the SmC* phase. Thus, the order parameter introduced to characterize the transition SmA$\rightarrow$SmC* is the angle of tilt θ. However, since these products are ferroelectric polarization appears locally in the sample. This polarization is connected to the tilt angle θ. We are then led to consider the polarization ($\boldsymbol{P}$) as a second order parameter. For a more detailed study that considers the helical structure in chiral smectic, a tensor order parameter Q must be considered. This parameter is zero in the disordered phase which is usually obtained at a high temperature, and non-zero in the ordered phase.

In order to describe the behavior of the system near the transition temperature, we develop the Landau free energy as a series of powers of coefficients of the order parameter.

3.1.1. The electro-clinic effect

By applying an electric field E to a liquid crystal sample presenting the SmA phase, an inclination of the director in the plane perpendicular to the electric field appears. The induced tilt angle is proportional to the amplitude of the applied electric field. This is called the electroclinic effect.[18]

For a linear treatment of the electro-clinical effect, Marcerou and Dupon[7,18] described the free energy by taking into account only the dominant terms and the additional terms of the coupling between the electric field and the induced polarization P. They kept only the terms of the lowest order in the expression of the energy

$$F = \frac{1}{2}a\theta^2 + \frac{1}{2\chi_\perp}P^2 - cP\theta PE - \frac{\varepsilon_\perp}{2}E^2. \quad (17)$$

In the absence of an electric field at the equilibrium, we have $\partial F/\partial\theta = 0$ and $\partial F/\partial P = 0$, which gives $P = 0$ and $\theta = 0$, corresponding to the SmA phase.

If an electric field "E" is applied in a direction parallel to the plane of the layers, at the equilibrium, we have

$$\theta = \frac{\chi_{\perp C}}{a^*}E, \quad P_{\text{ec}} = \frac{\chi_{\perp_\perp C^2}}{a^*}E, \quad (18)$$

where $a^* = \alpha(T - T_c^*)$ and $T_c^* = T_c + \frac{(\chi_\perp C^2)}{\alpha}$. These relations are linear with respect to the applied electric field.

It should be noted that the electro-clinical effect also exists in the low-temperature phase, near the transition temperature SmA* $\rightarrow$ SmC*, but the latter is masked by the spontaneous inclination in the tilt phase.

3.2. Empiric correction and field induced phase transitions

Although the Landau De-Gennes model allows for a description of certain electric phenomena such as spontaneous polarization and the electro-clinic effect by taking into consideration the applied electric field, it is unable to describe field induced phase transitions.

In the (E–T) diagram, the boundaries between the domains show a dependence of the threshold field as a function of temperature. It is therefore necessary to correct the previous development in order to be able to describe these transitions.

We propose in the following an empirical correction, which was deduced from experimental results, in order to locate the boundaries between the domains of the (E–T) diagram in the vicinity of the SmA–SmC$^*_\alpha$ transition. This correction affects the mean field term of the Landau De-Gennes development of the free energy. In this process, we write the temperature of the transitions T_c as a quadratic function of the applied electric field.

3.2.1. Expression of the free energy

For the SmA phase, the phase tilt angle θ and the polarization are both zero. In the SmC$^*_\alpha$ phase the precession of the molecules around the angle normal to the layers is very fast. The medium behaves as uniaxial and the tilt angle of this phase has a zero average, similar to that of the SmA phase. If we apply an electric field to the SmC$^*_\alpha$ phase, this results in helix destruction and an induced polarization. We can then speak of the appearance of an apparent tilt angle as in the electro-clinic effect.

To study the field-induced transition $SmC^*_\alpha \rightarrow SmC^*_{unwound}$ we can assume that this transition can be treated with the same formalism used for the $SmA^* \rightarrow SmC^*_\alpha$ transition induced by temperature variation.

In the free energy expression we propose a slight correction of the mean field term as follows: $a = \alpha(T - T_c)$, in which we write T_c as a function of the applied field "E".

$$T_c = T_c^* - \beta\left(E^2 - E_c^{*2}\right), \tag{19}$$

where T_c^* and E_c^* are the coordinates of the triple point "C" (Fig. 1).

The choice of the quadratic form means that the two orientations $+E$ and $-E$ are equivalent.

For $E = 0$ we find the transition temperature $SmA^* \rightarrow SmC^*_\alpha$ as

$$T_c(0) = T_c^* + \beta E_c^{*2} = T_{c0}. \tag{20}$$

We then express the free energy as Eq. (17). Minimizing with respect to θ and P gives: at zero field, in the SmC^*_α phase, $P = 0$ and $\theta = 0$.

Under an electric field ($E \neq 0$), as in the electro-clinic effect, we have

$$\begin{cases} \alpha\left[(T - T_c^*) + \beta(E^2 - E_c^{*2})\right]\theta = cP, \\ P = \chi_\perp\left[E + C\theta\right] = P_{die} + P_{elec}, \end{cases} \tag{21}$$

which gives

$$\begin{cases} \theta = \dfrac{c\chi_\perp}{\alpha(T - T_c^*) - \alpha\beta E_c^{*2} - c^2\chi_\perp + \alpha\beta E^2}E, \\ P_{elec} = \dfrac{\chi_\perp^2 c^2}{\alpha(T - T_c^*) - \alpha\beta E_c^{*2} - c^2\chi_\perp + \alpha\beta E^2}E. \end{cases} \tag{22}$$

For the first order we find a linear behavior. A non-linearity appears for high values of the applied electric field.

3.2.2. The SmA^*–SmC^*_α transition

For a fixed value of the electric field "E", the transition SmA^* and SmC^*_α takes place at the temperature given by

$$T_c = T_c^* - \beta\left(E^2 - E_c^{*2}\right) = T_{c0} - \beta E^2. \tag{23}$$

The boundary separating the two domains SmA^* and SmC^*_α has a parabolic shape (Fig. 1). The experimental observation of the (E,T) diagram shows a curve which has a pattern corresponding to a positive value of the parameter β ($\beta > 0$). We adopt this sign of β in the following analysis.

Note that for this transition we have $E \leq E_c^*$.

3.2.3. The SmC^*_α–$SmC^*_{unwound}$ transitions

For a fixed value of the temperature T, the transition SmC^*_α–$SmC^*_{unwound}$ takes place at the value of the applied electric field such that

$$E = \sqrt{\frac{T_c^* - T}{\beta} + E_c^{*2}} = \sqrt{\frac{T_{c0} - T}{\beta}}. \tag{24}$$

Note that for this transition we have $T \leq T_c^*$.

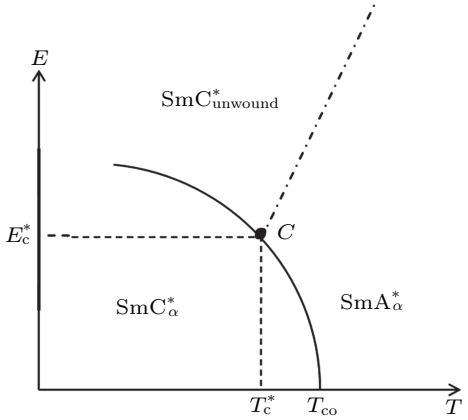


Fig. 1. Shape of the boundary separating the domains SmA^*–SmC^*_α and SmC^*_α–$SmC^*_{unrolled}$ in the (E,T) phase diagram for $\beta > 0$.

4. Comparison with experiment

In the following analysis, we present an experimental validation of the previous classical thermodynamic study and the empirical correction.

4.1. The (E,T) phase diagram

The (E,T) phase diagram of the chiral smectic compounds $C_{10}F_3$ is presented, which presents only the non-polar phases at zero fields (Fig. 2). The wide temperature range of the SmC^*_α phase facilitates the conduction of experiments.

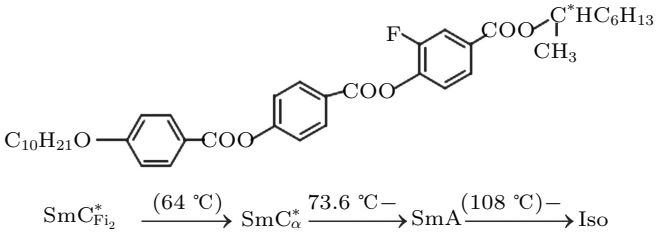


Fig. 2. Chemical formula and phase sequence at zero field of the compound $C_{10}F_3$.

Under an applied electric field, the helical structure is distorted. For strong fields, there is a total destruction of this structure and the product transitions to the unwound $SmC^*_{unwound}$ phase. This transition can occur directly as in the case of the SmC^*_α phase or in two stages as in the case of SmC^*_{Fi2}, where the sample transitions through an intermediate ferrielectric state (Fig. 3).

This diagram is the result of several techniques including the constant current method (squares), electro optical method (circles) and the method of dielectric spectroscopy (triangles).[7] Several works dealing with experimental studies of the (E,T) phase diagram of the product $C_{10}F_3$ have been previously published.[7,9] The curve of Fig. 4 represents the time dependence of the cell voltage following the injection of a constant current of 5 nA. The plate in the center indicates a coexistence between the initial phase SmC^*_α and that obtained at the strong field $SmC^*_{unwound}$.

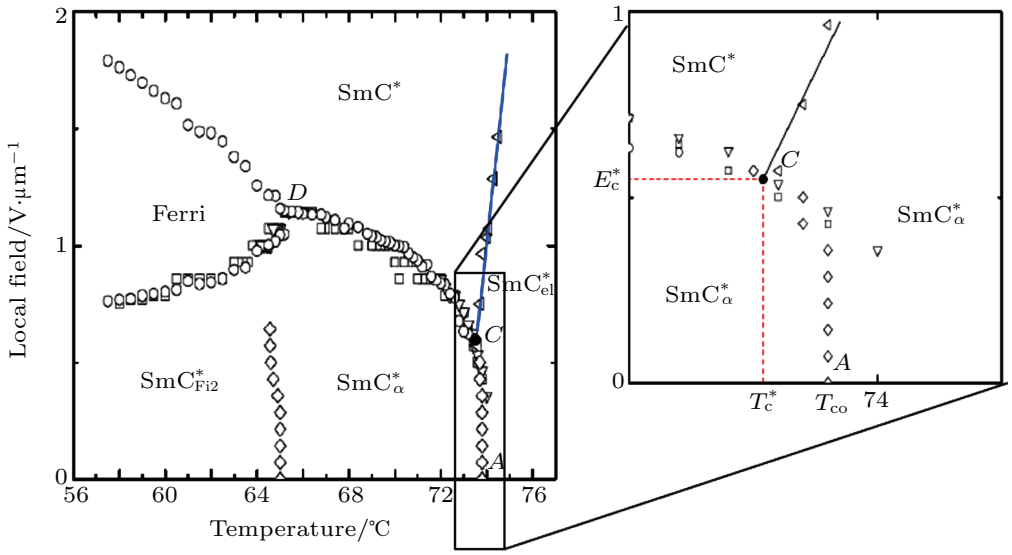


Fig. 3. (color online) (E,T) phase diagram of the compound $C_{10}F_3$ with zoom in the vicinity of the SmA–SmC$^*_\alpha$ transition temperature T_{co}.

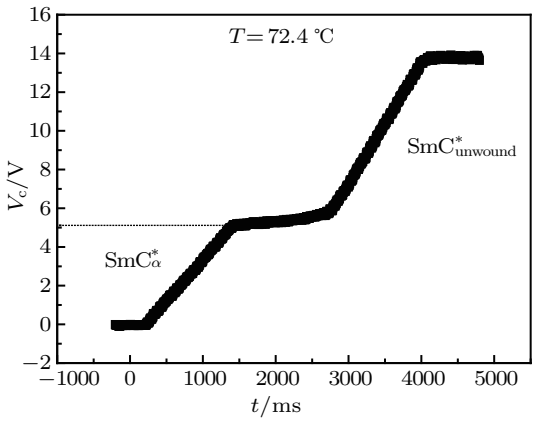


Fig. 4. Time dependence of V_c (constant current signal) for the product $C_{10}F_3$ with a cell thickness of 5 μm and a constant current intensity of 5 nA. The plate in the center indicates coexistence between the initial phase SmC$^*_\alpha$ and that obtained at strong field SmC$^*_{unwound}$.

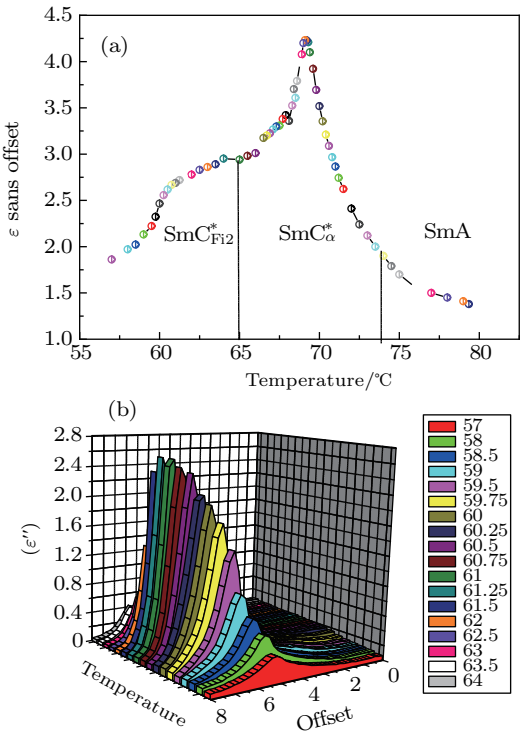


Fig. 5. (color online) (a) Temperature dependence of the module of dielectric permittivity at 200 Hz (without offset); (b) 3D plot of the imaginary part ε'' of the dielectric permittivity versus temperature. The cell thickness is 5 μm.

The curves of Figs. 5(a) and 5(b) are the results of a spectroscopy dielectric study without offset (a) and with offset (b). The peaks indicate an increase in the amplitude of the goldstone mode in the SmC$^*_\alpha$ phase. The beginning of the peak and its end mark the transitions SmA–SmC$^*_\alpha$ and SmC$^*_\alpha$–SmC$^*_{Fi2}$.

Two triple points are presented in Fig. 3. The first is the point C (E^*_c, T^*_c). The second is the point D. The boundary separating the SmC$^*_\alpha$ and SmC$^*_{unwound}$ domains takes the form of a parabolic branch.

The coordinates of the triple point "C" are: $T^*_c = 73.4$ °C and $E^*_c = 0.625$ V·μm^{-1}.

These values allow us to calculate the value of the parameter β.

Indeed, with $T_c* + \beta E^{*2}_c = T_{c0}$ and $T_{co} = 73.8$ °C, we have

$$\beta = \frac{T_{c0} - T^*_c}{E^{*2}_c} = \frac{0.4}{(0.625)^2} = 0.64 \times 10^{-12}\ \mathrm{K\cdot m\cdot V^{-1}}.$$

4.2. The SmC$^*_\alpha \rightarrow$ SmC$^*_{unwound}$ boundary

4.2.1. In the vicinity of the point C

The empirical correction makes it possible to trace this boundary in full, if we know the threshold fields of the SmC$^*{}_\alpha \rightarrow$ SmC$^*{}_{unwound}$ transition at two different temperatures. The coordinates of the triple point "C" and the value of the parameter β can be determined from Eq. (24). Then, we perform electro-optical measurements to monitor the variation of the spontaneous polarization according to the applied elec-

tric field, at two different temperatures. The threshold field for this transition corresponds to the change in the shape of the curve $P = f(E)$ (Fig. 6).

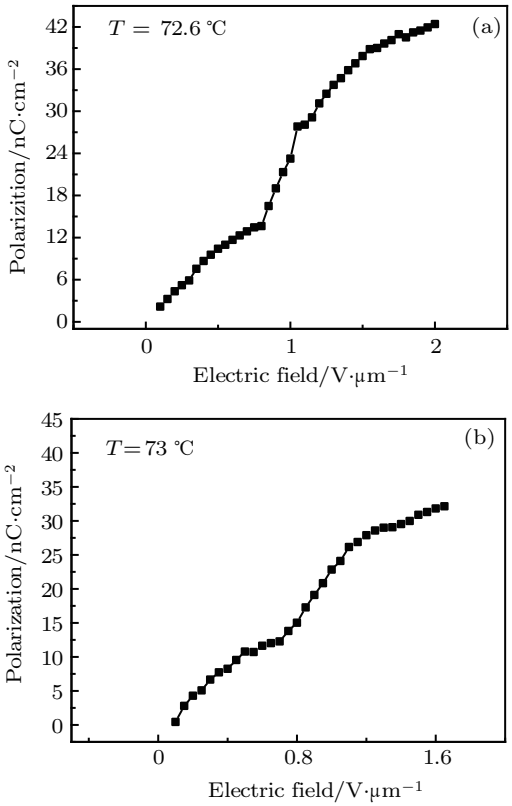


Fig. 6. (color online) Electro-optical effect in the SmC^*_α phase. The observed change in the shape of the curve in this plot indicates a phase transition under the applied field to the $SmC^*_{unwound}$ structure.

4.2.2. In the vicinity of the point D

In the temperature range [66 °C, 70 °C], the product $C_{10}F_3$ presents the SmC^*_α phase. A single transition towards the $SmC^*_{unwound}$ phase occurs when the threshold field value is reached. It should be noted that the dielectric permittivity ε has the highest value in the SmC^*_α phase. To study the (SmC^*_α–$SmC^*_{unwound}$) transition, we use the formula given in Eq. (16). Thus, we have

$$\alpha = \frac{E}{2\Delta\varepsilon}\left(\frac{\Delta\varepsilon}{\partial T}\right)_V. \tag{25}$$

To obtain the boundary delimiting the $SmC^*\alpha$ and $SmC^*_{unwound}$ domains, we plot the curve representing $\Delta\varepsilon = \varepsilon_1 - \varepsilon_2$ as a temperature function in the range [66 °C, 70 °C] as shown in Fig. 7. Noting that ε_1 and ε_2 were measured using the constant current method improved by Dhaouadi *et al.*,[9] figures 7(a) and 7(b) show the variations of ε_2 and ε_1 as a function of temperature, and of $\Delta\varepsilon$ in the region of interest of the study.

Based on the representative plot of the variation of the relative dielectric constant $\Delta\varepsilon$, we obtained the plot of the curve $\alpha = \frac{E}{2\Delta\varepsilon}\frac{\mathrm{d}(\Delta\varepsilon)}{\mathrm{d}T} = f(T)$ in Fig. 8.

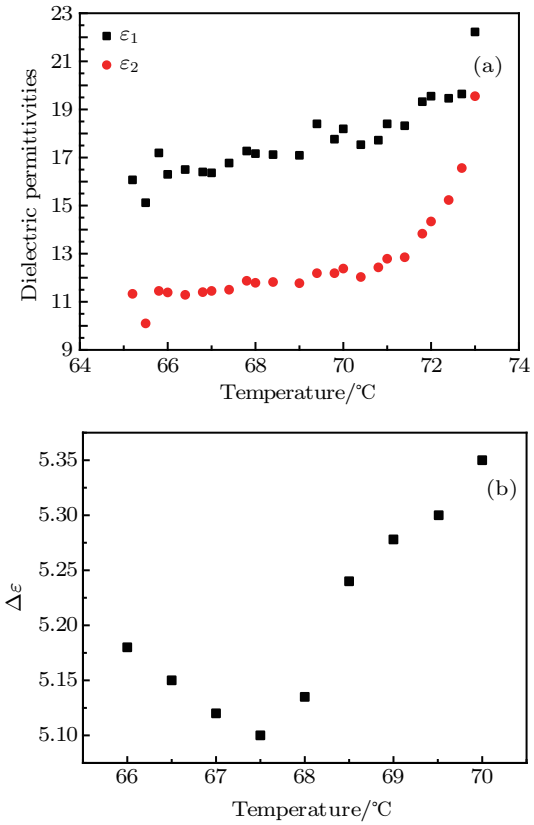


Fig. 7. (color online) (a) Representative curve of the relative dielectric constants ε_r in the $SmC^*_{unwound}$ phase in red and SmC^*_α in black. (b) Representative curve of $\Delta\varepsilon = \varepsilon_1 - \varepsilon_2$ in the range of temperature [66 °C, 7 °C].

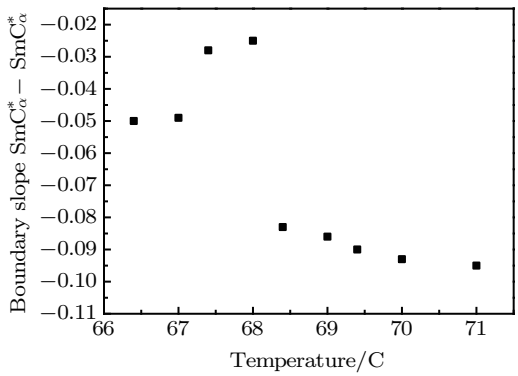


Fig. 8. (color online) Curve representing the variation of the slope $\alpha(T)$ of the $SmC^*_\alpha \rightarrow SmC^*_{unwound}$ boundary.

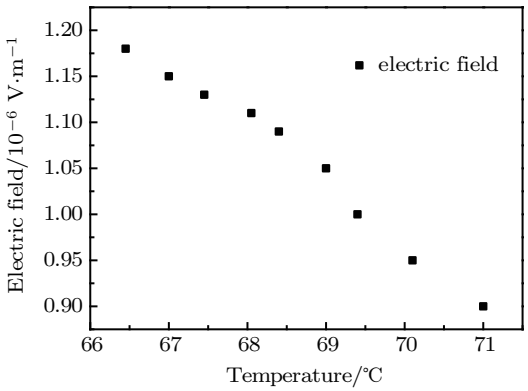


Fig. 9. (color online) Curve $E = f(T)$ representing the boundary which separates the two domains $SmC^*_\alpha \rightarrow SmC^*_{unwound}$.

Noting that the slope α is always negative, this demonstrates a decreasing boundary similar to that of Fig. 3. In Fig. 9 we trace this boundary from the previous results.

5. Conclusion

In this work, we investigated the borders between the domains of chiral smectic mesophases in (E,T) phase diagrams. By deriving an appropriate thermodynamic potential for ferroelectric materials, we analyzed the equilibrium state of the system during transitions under an applied electric field. During these transitions, two phases coexist, and the equilibrium of the system is translated by the equality of the thermodynamic potentials that correspond to each of the two phases. This equality makes it possible to revisit the expression of the slope $\alpha = (\mathrm{d}E/\mathrm{d}T)$ of the curve joining two domains in the (E,T) diagram, as a function of temperature.

To explain the shape of the domain border near the SmA–SmC^*_α transition, we introduce an empirical correction to the Landau De-Gennes development of the free energy. This correction facilitates the study of field induced phase transitions using the Landau De-Gennes theory.

In further investigations, we will extend this study to include the more complex case corresponding to the temperature range [57 °C, 64 °C], where the product $C_{10}F_3$ presents the $\mathrm{SmC}^*_{\mathrm{Fi2}}$ phase. Two field-induced phase transitions are observed in such a case as the sample transitions first to an intermediate polar state before a final transition to the $\mathrm{SmC}^*_{\mathrm{unwound}}$ phase under a strong field.

References

[1] Clark N and Lagerwall S T 1980 *Appl. Phys. Lett.* **36** 899

[2] Chandani A D L, Gorecka E, Ouchi Y, Takezoe H and Fukuda A 1989 *Jpn. J. Appl. Phys.* **28** L1265

[3] Cady A and al 2001 *Phys. Rev. E* **64** 050702R

[4] Hirst L S and al 2002 *Phys. Rev. E* **65** 041705

[5] Dhaouadi H 2009 *Phys. Rev. E* **80** 031712

[6] Wang S, Pan L D, Pindak R, Liu Z Q, Nguyen H T and Huang C C 2010 *Phys. Rev. Lett* **104** 027801

[7] Marcerou J P, H. Nguen T, Bitri N, Gharbi A, Essid S and Soltani T 2007 *Eur. Phys. J* **23** 319

[8] Riahi O, Trabelsi F, Dhaouadi H, Zgueb R and Othman T 2016 *Phase Transitions*

[9] Dhaouadi H, Zgueb R, Riahi O and al 2016 *Chin. Phys. B* **25** 057704

[10] Hamaneh M B and Taylor P L 2005 *Phys. Rev. E* **72** 021706

[11] Rjili M, Gharbi A, Othman T and al 2014 *Phys. Rev. E* **89** 022507

[12] Gleeson H Fand Hirst L S 2006 *ChemPhysChem* **7** 321

[13] Jaradet S, Brimicombe P D, Osipov M A, et al. 2011 *App. Phys. Lett.* **98** 043501

[14] Zgueb R, Dhaouadi H and Othman T 2014 *Liq. Cryst.* **41** 1394

[15] Soltani T, Marcerou J P and Othman T 2016 *Journal of Molecular Liquids* **215** 110

[16] Landau L, Lifshitz L and Pitaevsky L P 1984 *Electrodynamics of Continuous Media,* 2nd ed. (Oxford: Pergamon Press)

[17] De Gennes P G 1974 *The Physics of Liquid Crystals* (Oxford: Clarendon Press)

[18] Dupont L, Glogarova M, Marcerou J P, Nguyen H T, Destrade C and Lejcek L 1991 *Phys. II. France* **1831** 844

[19] Manai M, Gharbi A, Essid S, Achard M F, Marcerou J P, Nguyen H T and Rouillon J C 2006 *Ferroelectrics* **343** 27

[20] Jack C Burfoot 1967 *Ferroelectrics: An Introduction to the Physical Principles* (Princeton, New Jersey: Butler & Tanner LTD)

[21] Blinc R 1976 *Ferroelectrics* **14** 603

[22] Idenbom V L, Pikin S A and Loginov E B 1976 *Kristallografiya* **21** 1093; *Sov. Phys. Crystallogr.* **21** 632